

Atypical kinetics of cytochromes P450 catalysing 3'-hydroxylation of flavone from the white-rot fungus *Phanerochaete chrysosporium*

Received July 24, 2009; accepted September 3, 2009; published online October 9, 2009

Noriyuki Kasai¹, Shinichi Ikushiro¹,
Shinji Hirosue², Akira Arisawa²,
Hirofumi Ichinose³, Yujirou Uchida³,
Hiroyuki Wariishi³, Miho Ohta⁴ and
Toshiyuki Sakaki^{1,*}

¹Department of Biotechnology, Faculty of Engineering, Toyama Prefectural University, 5180 Kurokawa, Imizu, Toyama 939-0398;

²Bioresource Laboratories, Mercian Corp., Iwata-shi, Shizuoka;

³Department of Forest and Forest Products Sciences, Graduate School of Bioresource and Bioenvironmental Sciences, Kyushu University, Fukuoka 812-8581; and ⁴Department of Food and Nutrition Management Studies, Faculty of Human Development, Soai University, 4-4-1 Nanko-naka, Suminoe-ku, Osaka 559-0033, Japan.

*Toshiyuki Sakaki, Department of Biotechnology, Faculty of Engineering, Toyama Prefectural University, 5180 Kurokawa, Imizu, Toyama 939-0398, Japan. Tel: +81 766 56 7500, Fax: +81 766 56 2498, E-mail: tsakaki@pu-toyama.ac.jp

We cloned full-length cDNAs of 130 cytochrome P450s (P450s) derived from *Phanerochaete chrysosporium* and successfully expressed 70 isoforms in *Saccharomyces cerevisiae*. To elucidate substrate specificity of *P. chrysosporium* P450s, we examined various substrates including steroid hormones, several drugs, flavonoids and polycyclic aromatic hydrocarbons using the recombinant *S. cerevisiae* cells. Of these P450s, two CYPs designated as PcCYP50c and PcCYP142c with 14% identity in their amino acid sequences catalyse 3'-hydroxylation of flavone and *O*-deethylation of 7-ethoxycoumarin. Kinetic data of both enzymes on both reactions fitted not to the Michaelis–Menten equation but to Hill's equation with a coefficient of 2, suggesting that two substrates bind to the active site. Molecular modelling of PcCYP50c and a docking study of flavone to its active site supported this hypothesis. The enzymatic properties of PcCYP50c and PcCYP142c resemble mammalian drug-metabolizing P450s, suggesting that their physiological roles are metabolism of xenobiotics. It is noted that these unique *P. chrysosporium* P450s have a potential for the production of useful flavonoids.

Abbreviations: CYP, cytochrome P450; DCDD, dichloro-dibenzo-*p*-dioxin; DD, dibenzo-*p*-dioxin; 7-EC, 7-ethoxycoumarin; 7-HC, 7-hydroxycoumarin; MCDD, monochloro-dibenzo-*p*-dioxin.

White-rot fungi are capable of degrading a wide variety of recalcitrant aromatic compounds, including polymeric lignin and environmentally persistent pollutants. Cytochrome P450-mediated oxygenation

reactions play an important role during fungal metabolism of recalcitrant xenobiotic compounds as described previously (1). A whole genomic sequence of *Phanerochaete chrysosporium* revealed the presence of 148 P450 genes (2). In previous studies, we demonstrated that *P. chrysosporium* P450s have diverse and unique functions using a series of well-characterized P450 substrates known for other organisms (3), and expressed enzymatically active *P. chrysosporium* P450 designated as PcCYP1f in *Pichia pastoris* (1).

Recently, we cloned full-length cDNAs of more than 130 *P. chrysosporium* P450s and successfully expressed 70 isoforms out of these P450s using a co-expression system with yeast NADPH-P450 reductase in *Saccharomyces cerevisiae*. To elucidate substrate specificity of *P. chrysosporium* P450s, we examined various substrate candidates including steroid hormones, several drugs and polycyclic aromatic hydrocarbons such as dioxins. In a previous study, we demonstrated that the recombinant *S. cerevisiae* cells expressing PcCYP65a2 catalyse 3'-hydroxylation of naringenin to yield eriodictyol that has pharmacologically useful properties. In addition, PcCYP65a2 metabolized polycyclic aromatic compounds such as dibenzo-*p*-dioxin (DD), 2-monochloroDD, biphenyl and naphthalene (4). These results suggest that PcCYP65a2 is practically useful for both bioconversion and bioremediation.

Flavonoids exhibit an array of pharmacological properties, including anti-anxiety effects (5), improvement of cardiac function after ischaemia (6) and anti-estrogenic effects in breast cancer cell cultures (7). Flavonoids exist only in a relatively small food group that includes parsley, thyme, celery and sweet red pepper (8). Thus, biosynthesis of these compounds from micro-organisms, similar to the biosynthesis that has been described before in the report of Leonard *et al.* (9) and references therein, can be a useful method in place of extraction from plants.

In this study, we focus on the P450s that act on flavone, the simplest form among the flavonoids. As a result of the screening, the recombinant *S. cerevisiae* cells expressing each of PcCYP50c and PcCYP142c showed a high hydroxylation activity towards flavone. Thus, we examined their enzymatic properties using a microsomal fraction prepared from the recombinant *S. cerevisiae* cells. Unexpectedly, kinetic studies of these P450s showed a sigmoidal behaviour. Atypical kinetics was observed in both PcCYP50c- and PcCYP142c-dependent flavone 3'-hydroxylation and 7-ethoxycoumarin-*O*-deethylation. We demonstrate a docking model of two molecules of flavone in the active site of PcCYP50c that supports the atypical kinetics.

Material and methods

Materials

Flavone and 7-hydroxycoumarin (7-HC) were purchased from Sigma-Aldrich (St Louis, MO, USA). 7-Ethoxycoumarin (7-EC) was purchased from Nacalai Tesque (Kyoto, Japan) and from Sigma-Aldrich. NADPH was purchased from Oriental Yeast (Tokyo, Japan). All other chemicals were purchased from standard commercial sources and were of the highest quality available.

cDNAs cloning of PcCYP50c and PcCYP142c

PcCYP50c cDNA was obtained from *P. chrysosporium* cDNA library by PCR using primers (i) 5'-ATGCCAC TATTGCTCGTCGA-3' and (ii) 5'-GGTTCTATGCG TCCAAGCTG-3' for the entire coding region of PcCYP50c on the basis of PcCYP50c gene sequence (data not shown), and PcCYP142c cDNA was obtained by PCR using primers (i) 5'-ATGTGCTCT CTGCTTGTCTAGTCG-3' and 5'-CTACAGCGG AGTGACGTGCAG-3' for the entire coding region of PcCYP142c on the basis of PcCYP142c gene sequence (data not shown). Nucleotide sequences of PcCYP50c and PcCYP142c were confirmed by DNA sequencing.

Construction of expression plasmids for PcCYP50c and PcCYP142c

The expression plasmid for PcCYP50c was constructed as follows. The DNA fragment encoding PcCYP50c was amplified by PCR with primer combination of 5'-GCACTAGTAAAAAATGCCACTATTGCTC GTCG-3' and 5'-GCACTAGTCTATGCGTCCAAG CTGAAAATCTC-3', resulting in the generation of artificial SpeI restriction site at the ends of the PCR product. The PCR product was digested with SpeI and incorporated into the co-expression vector for P450 and yeast NADPH-P450 reductase, pGYR, digested with SpeI (10). *Saccharomyces cerevisiae* AH22 cells were transformed with the resultant plasmid named pG50c as described previously (10).

The expression plasmid for PcCYP142c was constructed in a similar manner. The DNA fragment encoding PcCYP142c was amplified by PCR with primer combination of 5'-GCAAGCTTAAAAAAT GTCGTCTCTGCTTGTCC-3' and 5'-GCAAGCTTC TACAGCGGAGTGACGTGCAGTGG-3', and the resultant DNA fragment was digested with HindIII, and then incorporated into the vector pGYR. *Saccharomyces cerevisiae* AH22 cells were transformed with the resultant plasmid named pG142c.

Metabolism of flavone in the culture of the recombinant *S. cerevisiae* cells expressing PcCYP50c or PcCYP142c and NADPH-P450 reductase

The recombinant *S. cerevisiae* cells expressing PcCYP50c or PcCYP142c were cultivated in a synthetic minimal medium containing 8% glucose, 5.4% yeast nitrogen base without amino acids and 160 mg/l histidine at 30°C. The substrate flavone (100 mM ethanol solution) was added to the cell culture at a final concentration of 0.1 mM. At 22 h after addition of the

substrate, the cell culture was vigorously mixed with four volumes of chloroform/methanol (3:1 v/v). The organic phase was recovered and dried in a vacuum evaporator centrifuge (Sakuma Seisakusyo, Tokyo, Japan). The resulting residue was solubilized with acetonitrile, and applied to HPLC under the following conditions: column, YMC-Pack ODS-AM (4.6 mm × 300 mm) (YMC, Kyoto, Japan); flow rate, 1.0 ml/min; UV detection, 290 nm; column temperature, 40°C; mobile phase, a linear gradient of 50–100% acetonitrile aqueous solution containing 0.01% trifluoroacetic acid per 10 min followed by 100% acetonitrile for 5 min.

LC-MS analysis of the metabolite produced by PcCYP50c

Isolated metabolites from HPLC effluents were subjected to mass spectrometric analysis, using a Finnigan LCQ ADVANTAGE MIX (ThermoFisher SCIENTIFIC, Waltham, MA, USA) with atmospheric pressure chemical ionization, positive mode. The conditions of LC were described below: column, reverse phase ODS column (2 mm × 150 mm, Develosil RPAQUEOUS-AR-5, Nomura Chemical Co. Ltd, Aichi, Japan); 30–80% methanol; flow rate, 0.2 ml/min; temperature, 40°C; UV detection, 290 nm.

¹H-NMR analysis of the metabolite produced by PcCYP50c

The 400 MHz ¹H-NMR spectra of the metabolite of flavone were measured on a BRUKER-400 (¹H, 400.1 MHz). The metabolite of flavone (40 µg) was dissolved in 500 µL of CDCl₃ and transferred into a probe. The time of domain data was multiplied with a squared sine-bell function.

Preparation of microsomal fractions from the recombinant *S. cerevisiae* cells

The recombinant *S. cerevisiae* AH22/pG50c or AH22/pG142c cells expressing PcCYP50c or PcCYP142c were cultivated in a synthetic minimal medium containing 8% glucose, 5.4% yeast nitrogen base without amino acids and 160 mg/l histidine. Microsomal fractions of AH22/pG50c or AH22/pG142c cells were prepared as described previously (10).

Measurement of reduced CO difference spectra

The reduced CO difference spectra were measured with a Hitachi U-3310 spectrophotometer with a head-on photomultiplier (Hitachi Co. Ltd, Tokyo, Japan), and the concentrations of PcCYP50c and PcCYP142c were determined from the reduced CO difference spectra using a difference of the extinction coefficients at 449 and 490 nm of 91 mM/cm (11, 12).

Measurement of flavone oxidation by microsomal fractions containing PcCYP50c or PcCYP142c

Microsomal fractions prepared from *S. cerevisiae* AH22/pG50c cells expressing PcCYP50c or AH22/pG142c cells expressing PcCYP142c were used for the metabolism of flavone. The substrate flavone was dissolved in dimethyl sulphoxide. The reaction mixture contains PcCYP50c (50 nM) or PcCYP142c (100 nM)

and 30–200 μM flavone for PcCYP50c or 50–800 μM for PcCYP142c in the 50 mM potassium phosphate buffer, pH 7.4. The reaction was initiated by the addition of 1 mM NADPH, and the reaction mixture was incubated at 37°C for 5 min for PcCYP50c or 10 min for PcCYP142c. Aliquots of the reaction mixture were extracted with four volumes of chloroform/methanol (3:1 v/v). The organic phase was recovered and analysed by HPLC as described above. As we have no authentic standard of 3'-hydroxyflavone, the same extinction coefficients at 290 nm as flavone is used to quantify 3'-hydroxyflavone.

Measurement of 7-EC O-deethylation by microsomal fractions containing PcCYP50c or PcCYP142c

Microsomal fractions prepared from *S. cerevisiae* AH22/pG50c cells expressing PcCYP50c or AH22/pG142c cells expressing PcCYP142c were used for metabolism of 7-EC. The substrate 7-EC was dissolved in dimethyl sulphoxide. The reaction mixture contains PcCYP50c (10 nM) or PcCYP142c (100 nM) and 50–600 μM 7-EC for PcCYP50c or 50–1250 μM for PcCYP142c in the 50 mM potassium phosphate buffer, pH 7.4. The reaction was initiated by the addition of 1 mM NADPH, and the reaction mixture was incubated at 37°C for 5 min for PcCYP50c or 10 min for PcCYP142c. Aliquots of the reaction mixture were extracted with four volumes of chloroform/methanol (3:1 v/v). The organic phase was recovered and dried in a vacuum evaporator centrifuge (Sakuma Seisakusyo, Tokyo, Japan). The resulting residue was solubilized with acetonitrile, and applied to HPLC under the following conditions: column, YMC-Pack ODS-AM (4.6 mm \times 300 mm) (YMC, Kyoto, Japan); flow rate, 1.0 ml/min; UV detection, 320 nm; column temperature, 40°C; mobile phase, a linear gradient of 10–40% acetonitrile aqueous solution containing 0.1% trifluoroacetic acid per 15 min followed by 40% acetonitrile for 5 min.

Kinetic data analysis

As the initial rate v versus substrate concentration S showed a sigmoidal curve, the data were analysed using Hill's equation [Equation (1)] (13):

$$v/E_0 = k_{\text{cat}} \cdot S^n / (K_s^n + S^n) \quad (1)$$

The data were also analysed by the cooperative single-enzyme model proposed by Korzekwa *et al.* (14) with two binding sites in which the product can be formed either from the single-substrate-bound form or from the two-substrate-bound form of the enzyme [Equation (2)]:

$$v/E_0 = \{(k_{\text{cat1}} \cdot S) / K_{\text{m1}} + (k_{\text{cat2}} \cdot S^2) / (K_{\text{m1}} \cdot K_{\text{m2}})\} / \{1 + S / K_{\text{m1}} + S^2 / (K_{\text{m1}} \cdot K_{\text{m2}})\} \quad (2)$$

This model was used because n was close to 2 in Hill's equation, suggesting homotropic cooperativity. However, if the enzyme shows no activity in the single-substrate-bound complex [$k_{\text{cat1}} = 0$ in Equation (2)],

Equation (2) is simplified as Equation (3):

$$v/E_0 = \{(k_{\text{cat2}} \cdot S^2) / (K_{\text{m1}} \cdot K_{\text{m2}})\} / \{1 + S / K_{\text{m1}} + S^2 / (K_{\text{m1}} \cdot K_{\text{m2}})\} \quad (3)$$

Kinetic parameters were calculated with the nonlinear regression analysis according to Equations (1), (2) and (3) using the program of Kaleida-Graph (Synergy Software, Reading, PA, USA). All results are expressed as the mean \pm SD of three experiments.

Substrate docking

Graphical manipulations were performed using Molecular Operating Environment (MOE) (Ryoka Systems Inc., Tokyo, Japan). We constructed a three-dimensional model of PcCYP50c by the replacement method using human CYP2C9 (PDF; 1OG2) as a template. Energy minimizations were performed using AMBER99 force field. The substrate, one flavone, was docked into the substrate-binding pocket by superposition with flavone in PcCYP50c, and another flavone was subsequently docked into the same pocket with one flavone in the same way. Each complex was minimized on MMFF94 \times force field.

Other methods

The protein concentration was determined by the method of Lowry *et al.* (15), using bovine serum albumin as a standard. A sequence alignment between PcCYP50c and PcCYP142c was produced with ClustalW software (<http://align.genome.jp/sit-bin/clustalw>).

According to the P450 Nomenclature Committee, PcCYP50c and PcCYP142c correspond to CYP5147A1 and CYP5136A1, respectively, although PcCYP142c does not contain Leu215 of CYP5136A1 that is predicted from its genome sequence (<http://drnelson.utmem.edu/Phanerochaete.P450s.htm>). In addition, PcCYP65a2 corresponds to CYP5138A1 (<http://drnelson.utmem.edu/Phanerochaete.P450s.htm>). However, the amino acid sequence of CYP5138A1 has several differences from that of PcCYP65a2 that is deduced from its cDNA sequence (4).

Results

Expression of PcCYP50c and PcCYP142c in the recombinant *S. cerevisiae* cells

The reduced CO difference spectra of whole cell and microsomal fractions of the recombinant *S. cerevisiae* cells expressing PcCYP50c and PcCYP142c showed peaks at \sim 449 nm indicating the presence of the active P450 (Fig. 1). The contents of PcCYP50c and PcCYP142c in the microsomal fraction were estimated to be 40 and 119 pmol/mg protein, respectively.

Metabolism of flavone by recombinant yeast cells expressing PcCYP50c or PcCYP142c

Metabolism of flavone was examined by the addition of flavone to the culture of the recombinant

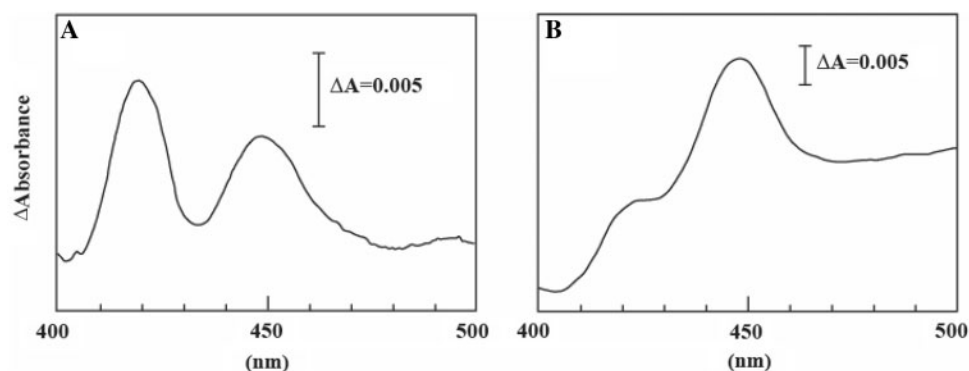


Fig. 1 Reduced CO difference spectra of microsomal fractions prepared from the recombinant *S. cerevisiae* AH22/pG50c cells (A) and AH22/pG142c cells (B). These spectra showed peaks at ~449 nm indicating the presence of active haem-containing P450 enzymes.

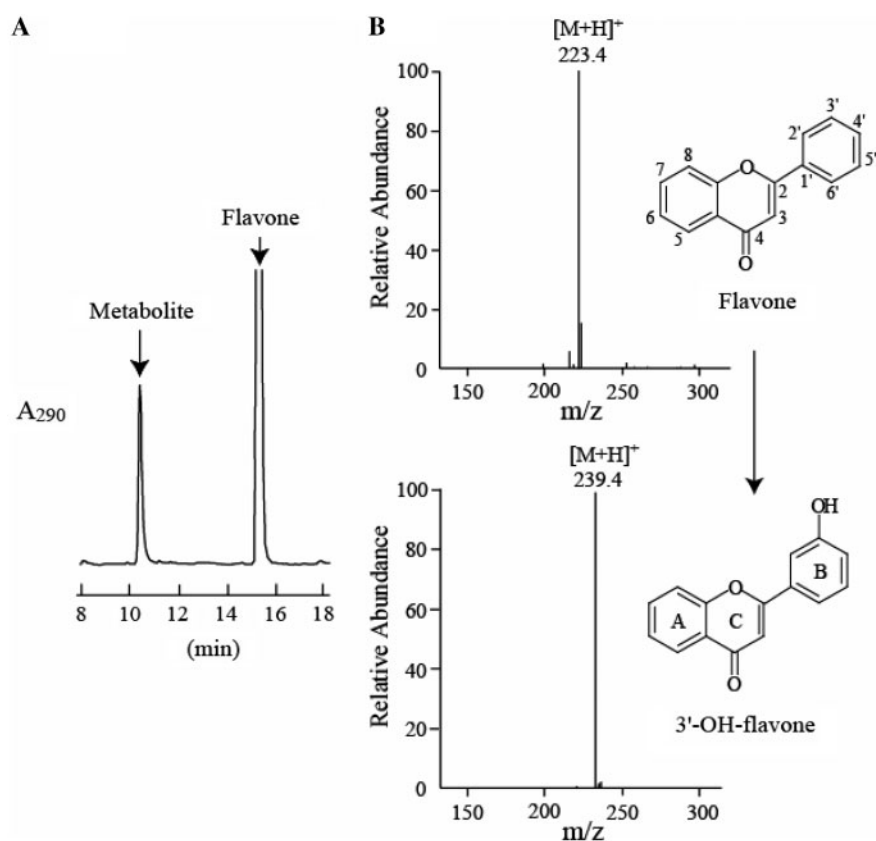


Fig. 2 HPLC profiles of flavone and its metabolite formed in the culture of the recombinant *S. cerevisiae* AH22/pG50c cells expressing *P. chrysosporium* CYP50c (A), and mass spectra of flavone and its metabolite by PcCYP50c (B). The metabolite was isolated from HPLC effluents and subjected to mass spectrometric analysis and NMR analysis. As a result, the metabolite appears to have a hydroxyl group as described in the Results section. Based on LC-MS and NMR analyses, the metabolite of flavone was identified as 3'-hydroxyflavone.

AH22/pG50c or AH22/pG142c cells. Figure 2 shows an HPLC profile of flavone and its metabolite by PcCYP50c after 22 h of incubation. Conversion ratio to the metabolite from flavone by PcCYP50c was ~10%. LC-MS analysis revealed that the molecular mass of the metabolite was 238 (flavone+O) (Fig. 2B). Metabolism of flavone by PcCYP142c was also examined in the same way, and the metabolite by PcCYP142c appears to be identical to that by PcCYP50c (data not shown).

¹H-NMR spectra of flavone and its metabolite

To identify the metabolite of flavone, we performed ¹H-NMR analysis of flavone and its metabolite. The resonances of hydrogen located in the A-ring of flavone were identified as follows: δ_{H} ppm (CDCl₃): 8.22 (1H, *dd*, $J=1.7, 7.9$ Hz, C-5), 7.69 (1H, *dt*, $J=1.7, 8.4$ Hz, C-7), 7.56 (1H, *d*, $J=8.3$ Hz, C-8), 7.41 (1H, *t*, $J=8.0$ Hz, C-6), 6.82 (1H, *s*, C-3). The resonances of hydrogen located in the B-ring of flavone were as follows: δ_{H} ppm

(CDCl₃): 7.92 (2H, *dd*, $J=2.7, 7.4$, C-2', C-6'), 7.53 (2H, *dt*, $J=1.6, 9.0$ Hz, C-3', C-5'), 7.51 (1H, *dt*, $J=1.5, 9.0$, C-4'). The resonances of hydrogen located in the A-ring of the metabolite were identified as follows: δ_{H} ppm (CDCl₃): 8.20 (1H, *dd*, $J=1.5, 8.0$ Hz, C-5), 7.69 (1H, *dt*, $J=1.7, 8.4$ Hz, C-7), 7.55 (1H, *d*, $J=7.8$ Hz, C-8), 7.41 (1H, *t*, $J=7.6$ Hz, C-6), 6.80 (1H, *s*, C-3). The resonances of hydrogen located in the B-ring of the metabolite were as follows: δ_{H} ppm (CDCl₃): 7.46 (1H, *d*, $J=8.3$ Hz, C-6'), 7.38 (1H, *d*, $J=2.1$ Hz, C-2'), 7.35 (1H, *t*, $J=7.9$ Hz, C-5'), 7.00 (1H, *ddd*, $J=0.86, 2.45, 8.1$ Hz, C-4'). Based on LC-MS and NMR analyses, the metabolite of flavone was identified as 3'-OH-flavone.

Kinetic analysis of flavone hydroxylation by PcCYP50c and PcCYP142c

Kinetic analysis of 3'-hydroxylation of flavone by recombinant PcCYP50c and PcCYP142c was carried out (Fig. 3). The v/E_0 -S plots showed sigmoidal curves, suggesting a positive cooperativity as described by Ueng *et al.* (16). Kinetic parameters of PcCYP50c with Hill's equation (equation 1), k_{cat} , n and K_s values, were calculated to be 0.52/min, 2.2 and 109 μM , respectively (Table 1). Kinetic parameters of PcCYP142c5 with Hill's equation (equation 1), k_{cat} , n and K_s values, were 0.019/min, 2.0 and 152 μM , respectively (Table 1). The kinetic data of PcCYP50c and PcCYP142c were also analysed by the two-substrate model (14, 16) using Korzekwa's equation

[Equation (2)]. However, $k_{\text{cat}1}$ value is negative when we use Equation (2). Thus, the kinetic parameters of PcCYP50c were calculated using Equation (3). The $k_{\text{cat}2}$, $K_{\text{m}1}$ and $K_{\text{m}2}$ values were 0.64/min, 235 μM and 50 μM , respectively (Table 1). The kinetic parameters of PcCYP142c5 with Equation (3), $k_{\text{cat}2}$, $K_{\text{m}1}$ and $K_{\text{m}2}$ values, were estimated to be 0.021/min, 219 μM and 71 μM , respectively (Table 1).

Kinetic analysis of 7-ethoxycoumarin O-deethylation by PcCYP50c and PcCYP142c

Kinetic analysis of O-deethylation of 7-EC by recombinant PcCYP50c and PcCYP142c was carried out in the same way as mentioned above (Fig. 4). The v/E_0 -S plots showed sigmoidal curves and kinetic parameters of PcCYP50c with Hill's equation [Equation (1)], k_{cat} , n and K_s values, were calculated to be 28/min, 1.8 and 222 μM , respectively (Table 1). Kinetic parameters of PcCYP142c with Hill's equation [Equation (1)], k_{cat} , n and K_s values, were 2.3/min, 2.3 and 684 μM , respectively (Table 1). The kinetic parameters of PcCYP50c with Equation (3), $k_{\text{cat}2}$, $K_{\text{m}1}$ and $K_{\text{m}2}$ values, were 33/min, 148 μM and 169 μM , respectively (Table 1). The kinetic parameters of PcCYP142c with Equation (3), $k_{\text{cat}2}$, $K_{\text{m}1}$ and $K_{\text{m}2}$ values, were 3.3/min, 1165 μM and 479 μM , respectively (Table 1).

Substrate docking

We constructed a three-dimensional model of PcCYP50c by the replacement method using human

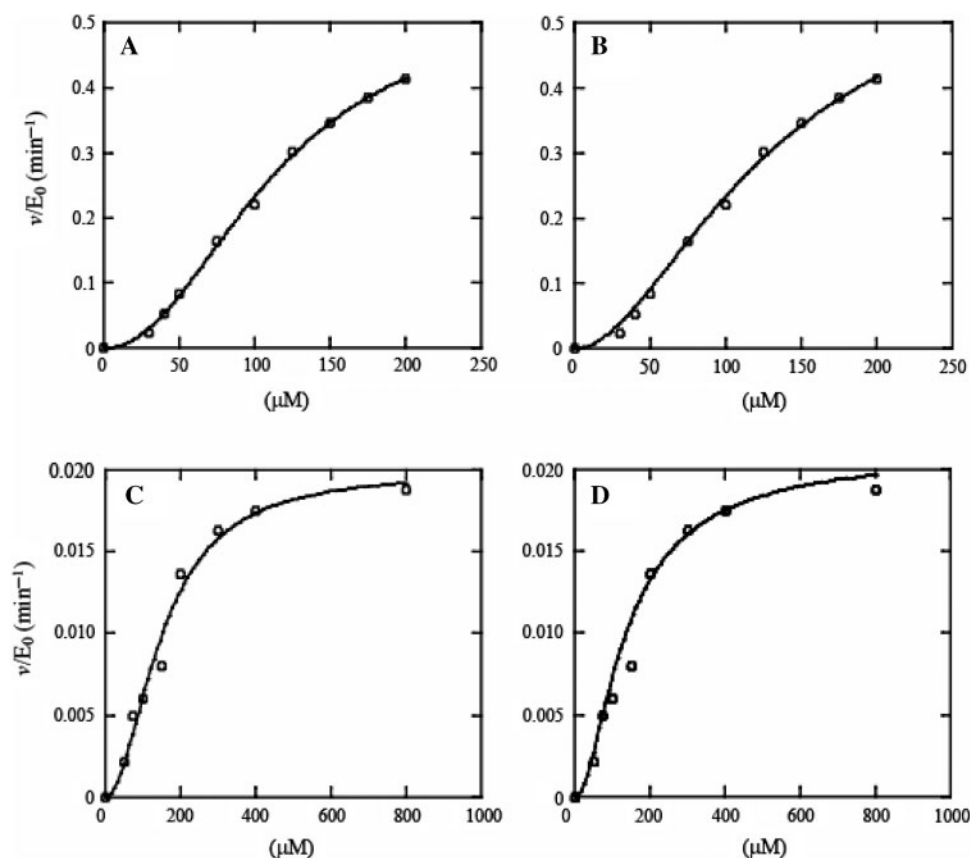


Fig. 3 Kinetic analysis of flavone 3'-hydroxylation by recombinant PcCYP50c (A and B) and PcCYP142c (C and D). The dots fitted to Hill's equation (A and C) and the two-substrate model equation (B and D).

Table 1. Kinetics parameters for conversion of flavone to 3'-OH-flavone and 7-EC to 7-HC in the microsomal fractions containing PcCYP50c or PcCYP142c.

Substrate	Hill equation			Two-substrate model, $k_{\text{cat}1} = 0$ equation		
	k_{cat} (min^{-1})	n	K_s (μM)	$k_{\text{cat}2}$ (min^{-1})	K_{m1} (μM)	K_{m2} (μM)
PcCYP50c						
Flavone	0.52 ± 0.03	2.2 ± 0.1	109 ± 6	0.64 ± 0.03	235 ± 10	50 ± 8
7-EC	28 ± 1	1.8 ± 0.1	222 ± 18	33 ± 1	148 ± 30	169 ± 25
PcCYP142c						
Flavone	0.019 ± 0.002	2.0 ± 0.4	152 ± 30	0.021 ± 0.002	219 ± 60	71 ± 34
7-EC	2.3 ± 0.1	2.3 ± 0.1	684 ± 35	3.3 ± 0.4	1165 ± 220	479 ± 93

The parameters represent means \pm SD from three separate experiments.

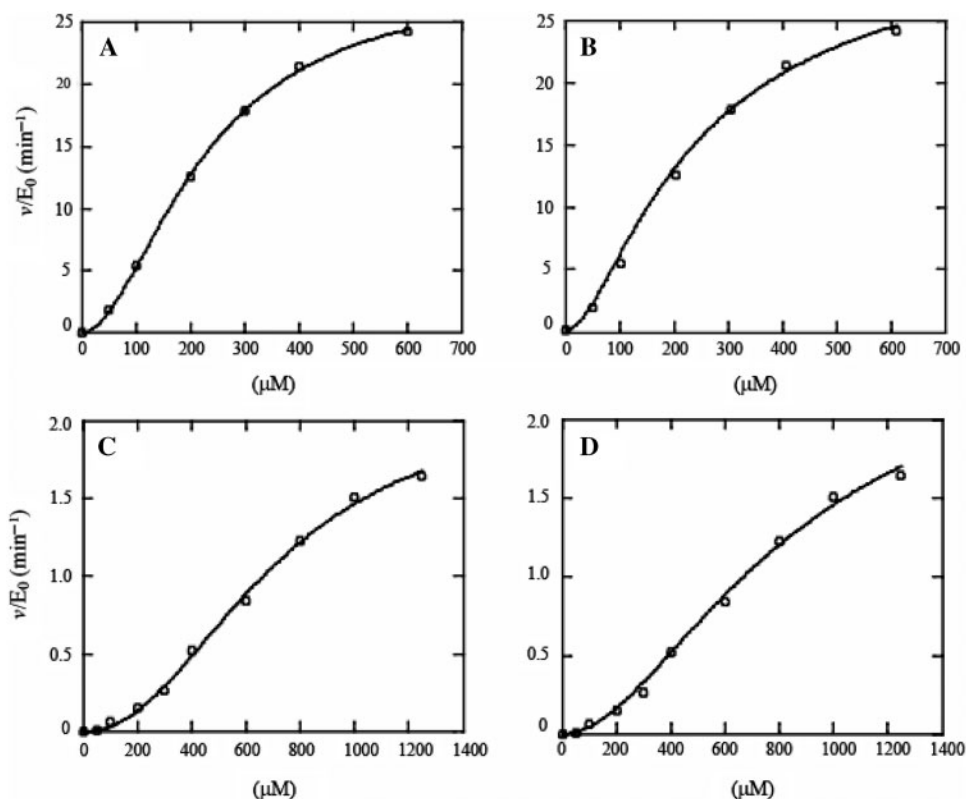


Fig. 4 Kinetic analysis of 7-EC *O*-deethylation by recombinant PcCYP50c (A and B) and PcCYP142c (C and D). The dots fitted to Hill's equation (A and C) and the two-substrate model equation (B and D).

CYP2C9 as a template, and docking simulation analyses were performed (Fig. 5). The homology of the amino acid sequences between PcCYP50c and human CYP2C9 was 25%. Based on the docking model, the distance between C-3' of firstly docked flavone and haem iron was 12.04 Å, which is too long for metabolism of flavone. On the other hand, the distance between C-3' of secondly docked flavone and haem iron was 5.37 Å, which is suitable for metabolism of flavone.

Discussion

As mentioned, white-rot fungi degrade a wide variety of recalcitrant aromatic compounds including polymeric lignin and environmentally persistent pollutants, where cytochrome P450-mediated oxygenation

reactions play an important role. Based on these results, it is possible to assume that aromatic compounds such as flavonoids are good substrates for some white-rot fungi P450s.

In a previous study, we found that one of the *P. chrysosporium* P450s, PcCYP65a2, shows hydroxylation activity towards naringenin and dioxins. PcCYP65a2 catalyses 3'-hydroxylation of naringenin to yield eriodictyol, which has various biological and pharmacological properties (4). In addition, PcCYP65a2 metabolized polyaromatic compounds such as dibenzo-*p*-dioxin (DD), 2-monochloroDD, biphenyl and naphthalene. These results suggest that white-rot fungi have some practically useful P450 genes (4).

In this study, we screened the P450s metabolizing flavone out of 70 *P. chrysosporium* P450s expressed

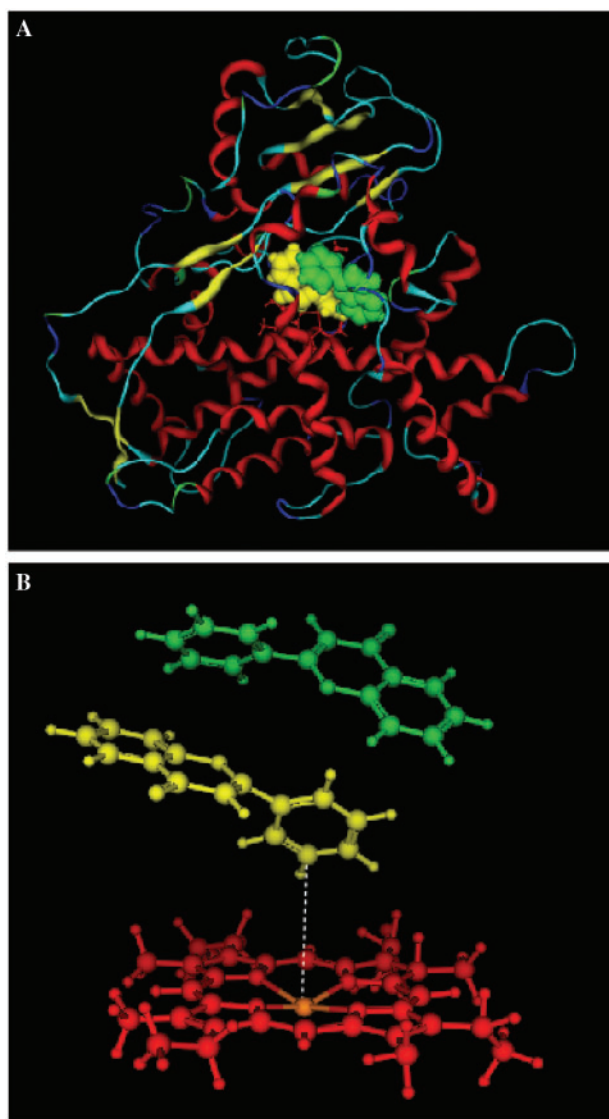


Fig. 5 Docking model of PcCYP50c and two flavones. (A) The whole structure of PcCYP50c docked with two flavones. Red skeleton, green and yellow compound represent the haem of PcCYP50c, first docked flavone and secondly docked flavone, respectively. Red and yellow ribbons represent helices and β -strands, respectively. (B) The interaction of the haem of PcCYP50c and two flavones in the substrate-binding pocket of PcCYP50c. Red skeleton, green compound and yellow compound represent the haem of PcCYP50c, first docked flavone and secondly docked flavone, respectively. The distance between C-3' of secondly docked flavone and haem iron is 5.37Å.

in *S. cerevisiae* cells, and found PcCYP50c and PcCYP142c which catalyse flavone 3'-hydroxylation. Figure 6 shows an alignment of amino acid sequences of PcCYP50c and PcCYP142c. The former has 20 hydrophobic amino acids at the amino terminus followed by basic amino acids and a Pro-rich region as well as most of the microsomal P450. However, PcCYP142c has only one Pro in this region. Both P450s have distal Thr and proximal Cys as a fifth axial ligand of haem iron. It is noted that PcCYP50c and PcCYP142c have only 14% amino acid sequence identity.

In spite of the low sequence similarity between PcCYP50c and PcCYP142c, they showed quite similar sigmoidal curves in the v/E_0 -S plots, suggesting the positive cooperativity as described by Ueng *et al.* (16). The Hill's constants were 2.2 and 2.0, suggesting that the binding of two substrates is needed for 3'-hydroxylation of flavone. To our best knowledge, this is the first report on P450s that shows positive cooperativity in the binding and hydroxylation of flavone. The k_{cat} value of PcCYP50c was much higher than that of PcCYP142c, while K_s values were similar. These results indicate that PcCYP50c is a better flavone hydroxylase than PcCYP142c. Kinetic data were also analysed by the two-substrate model. The assumption of $k_{cat1}=0$ was needed to use this model, suggesting no activity of PcCYP142c in the single substrate-bound complex. Based on these results, the docking model of flavone in the active site of PcCYP50c was constructed. The first flavone binds to the site where the distance between C-3' flavone and haem iron is 12.04Å, which is too long for metabolism of flavone. On the other hand, the distance between C-3' of secondly docked flavone and haem iron is 5.37Å, which is suitable for the metabolism of flavone. Thus, this model can readily explain the atypical kinetics of PcCYP50c.

Surprisingly, kinetic data of both PcCYP50c and PcCYP142c on 7-ethoxycoumarin *O*-deethylation also showed sigmoidal curves, suggesting that two 7-ethoxycoumarin molecules bind to the active sites of these P450s. Shimada *et al.* (17) reported kinetic parameters of *O*-deethylation of 7-EC by several human P450s; however, no atypical kinetics were reported therein. Thus, this study appears to be the first report on P450s that shows positive cooperativity in the binding and *O*-deethylation of 7-ethoxycoumarin. The K_s value of PcCYP50c in Hill's equation, and K_{m1} and K_{m2} values of PcCYP50c in the two-substrate model are significantly lower than those of PcCYP142c. On the other hand, k_{cat} and k_{cat2} values of PcCYP50c were much higher than those of PcCYP142c. These results demonstrate that PcCYP50c is a better 7-ethoxycoumarin *O*-deethylase than PcCYP142c.

It is well established that the active site of CYP3A4 contains two or more binding sites and can accommodate the simultaneous presence of at least two substrate molecules, or one substrate and an allosteric effector (18). Positive homotropic cooperativity with CYP3A4 substrates, with sigmoidal velocity curves, has been abundantly reported. Finally, the crystal structure of CYP3A4 revealed the presence of a peripheral binding site located above a phenylalanine cluster, which is involved in the initial recognition of substrates or allosteric effectors (19). Interestingly, flavone was reported to be an effective stimulator of CYP3A4 as measured by progesterone 6 β - and 16 α -hydroxylase activities (20). These facts suggest that enzymatic properties of PcCYP50c and PcCYP142c resemble those of CYP3A4. However, CYP3A4 hardly catalyses aromatic compounds. On the contrary, CYP1A2 acts on aromatic compounds well, but hardly shows atypical kinetics. Thus, it is

- flowers, is a central benzodiazepine receptors-ligand with anxiolytic effects. *Planta Med.* **61**, 213–216
6. Lebeau, J., Nevriere, R., and Cotellet, N. (2001) Beneficial effects of different flavonoids, on functional recovery after ischemia and reperfusion in isolated rat heart. *Bioorg. Med. Chem. Lett.* **11**, 23–27
 7. Miksicek, R.J. (1995) Estrogenic flavonoids: structural requirements for biological activity. *Proc. Soc. Exp. Biol. Med.* **208**, 44–50
 8. Ross, J.A. and Kasum, C.M. (2002) Dietary flavonoids: bioavailability, metabolic effects, and safety. *Annu. Rev. Nutr.* **22**, 19–34
 9. Leonard, E., Yan, Y., Lim, K.H., and Koffas, M.A. (2005) Investigation of two distinct flavone synthases for plant-specific flavone biosynthesis in *Saccharomyces cerevisiae*. *Appl. Environ. Microbiol.* **71**, 8241–8248
 10. Sakaki, T., Shinkyo, R., Takita, T., Ohta, M., and Inouye, K. (2002) Biodegradation of polychlorinated dibenzo-p-dioxins by recombinant yeast expressing rat CYP1A subfamily. *Arch. Biochem. Biophys.* **401**, 91–98
 11. Kondo, S., Sakaki, T., Ohkawa, H., and Inouye, K. (1999) Electrostatic interaction between cytochrome P450 and NADPH-P450 reductase: comparison of mixed and fused systems consisting rat cytochrome P4501A1 and yeast NADPH-P450 reductase. *Biochem. Biophys. Res. Commun.* **257**, 273–278
 12. Omura, T. and Sato, R. (1964) The carbon monoxide-binding pigment of liver microsomes: II. Solubilization, purification, and properties. *J. Biol. Chem.* **239**, 2379–2385
 13. Shou, M., Mei, Q., Ettore, M.W. Jr, Dai, R., Baillie, T.A., and Rushmore, T.H. (1999) Sigmoidal kinetic model for two co-operative substrate-binding sites in a cytochrome P450 3A4 active site: an example of the metabolism of diazepam and its derivatives. *Biochem. J.* **340**, 845–853
 14. Korzekwa, K.R., Krishnamachary, N., Shou, M., Parise, R.A., Rettie, A.E., Gonzalez, F.J., and Tracy, T.S. (1998) Evaluation of atypical cytochrome P450 kinetics with two-substrate models: evidence that multiple substrates can simultaneously bind to cytochrome P450 active sites. *Biochemistry* **37**, 4137–4147
 15. Lowry, O.H., Rosebrough, N.J., Farr, A.L., and Randall, R.J. (1951) Protein measurement with the folin phenol reagent. *J. Biol. Chem.* **193**, 265–275
 16. Ueng, Y., Kuwabara, T., Chun, Y., and Guengerich, F.P. (1997) Cooperativity in oxidations catalyzed by cytochrome P450 3A4. *Biochemistry* **36**, 370–381
 17. Shimada, T., Tsumura, F., and Yamazaki, H. (1999) Prediction of human liver microsomal oxidations of 7-ethoxycoumarin and chlorzoxazone with kinetic parameters of recombinant cytochrome P-450 enzymes. *Drug Metab. Dispos.* **27**, 1274–1280
 18. Oda, Y. and Kharasch, E.D. (2001) Metabolism of levo-alpha-Acetylmethadol (LAAM) by human liver cytochrome P450: involvement of CYP3A4 characterized by atypical kinetics with two binding sites. *J. Pharmacol. Exp. Ther.* **297**, 410–422
 19. Williams, P.A., Cosme, J., Vinkovic, D.M., Ward, A., Angove, H.C., Day, P.J., Vonrhein, C., Tickle, J.I., and Jhoti, H. (2004) Crystal structures of human cytochrome P450 3A4 bound to metyrapone and progesterone. *Science* **305**, 683–686
 20. Harlow, G.R. and Halpert, J.R. (1997) Alanine-scanning mutagenesis of a putative substrate recognition site in human cytochrome P450 3A4. Role of residues 210 and 211 in flavonoid activation and substrate specificity. *J. Biol. Chem.* **272**, 5396–5402